Environ Sci Pollut Res (2012) 19:3688–3695
DOI 10.1007/s11356-012-0932-y

Transition metal-modified zinc oxides for UV and visible light photocatalysis

J. Z. Bloh · R. Dillert · D. W. Bahnemann

Received: 30 January 2012 / Accepted: 12 April 2012

Abstract In order to use photocatalysis with solar light, finding more active and especially visible light active photocatalysts is a very important challenge. Also, studies of these photocatalysts should employ a standardized test procedure so that their results can be accurately compared and evaluated with one another. A systematic study of transition metal-modified zinc oxide was conducted to determine whether they are suitable as visible light photocatalysts. The photocatalytic activity of ZnO modified with eight different transition metals (Cu, Co, Fe, Mn, Ni, Ru, Ti, Zr) in three different concentrations (0.01, 0.1, and 1 at.%) was investigated under irradiation with UV as well as with visible light. The employed activity test is the gas-phase degradation of acetaldehyde as described by the ISO standard 22197-2. The results suggest that the UV activity can be improved with almost any modification element and that there exists an optimal modification ratio at about 0.1 at.%. Additionally, Mn- and Ru-modified ZnO display visible light activity. Especially the Ru-modified ZnO is highly active and surpasses the visible light activity of all studied titania standards. These findings suggest that modified zinc oxides may be a viable alternative to titanium dioxide-based catalysts for visible light photocatalysis. Eventually, possible underlying mechanisms are proposed and discussed.

Responsible editor Philippe Garrigues

J. Z. Bloh · R. Dillert · D. W. Bahnemann (✉)
Institut für Technische Chemie, Leibniz Universität Hannover,
Callinstr. 3,
30167 Hannover, Germany
e-mail: bahnemann@iftc.uni-hannover.de
URL: http://www.tci.uni-hannover.de

J. Z. Bloh
e-mail: bloh@iftc.uni-hannover.de

Keywords Photocatalysis · Zinc oxide · Visible light · Acetaldehyde degradation · ISO 22197-2

Introduction

Typical photocatalysts, such as titanium dioxide and zinc oxide, can only utilize ultraviolet light (Herrmann 2005). This disadvantage severely limits their application in both indoor and solar light situations. Therefore, the development of visible light active photocatalysts has been the focus of intensive research in the past years. Most of the efforts were focused on titanium dioxide, since it offers many advantageous properties and a high activity. These efforts led to the development of several commercial-grade visible light photocatalysts, based on N-, C-, or S-doping or modification with transition metal cations such as Fe^{3+}. Their efficiencies, however, are still too low for many applications (Rehman et al. 2009). Since titanium dioxide has already been studied so extensively without a suitable candidate emerging, some researchers are now looking at other materials that have not been as thoroughly studied and may have yet undiscovered potential. Therefore, this study investigates zinc oxide as a possible alternative.

Zinc oxide has already been modified or doped with transition metals such as Co (Xiao et al. 2007), Mn (Ullah and Dutta 2008; Zhang 2012), Ni (Ekambaram et al. 2007), and Cu (Kanade et al. 2007). However, each of those studies used different synthesis routes and methods to determine the activity, making it impossible to compare and evaluate these results with one another and with those of titanium dioxide. In order to achieve comparability between the results of different researchers, it is of paramount importance that the applied activity tests are standardized. To the best of our knowledge, no comprehensive study of transition metal-

modified zinc oxide was conducted with a standardized test that would enable to properly compare the obtained results. For this reason, the activity test utilized in this study was the standardized gas-phase acetaldehyde degradation, as described by the ISO standard 22197-2.

In this work, we present the results of a systematic study of zinc oxide modified with eight different transition metals in at least three concentrations each with the aim of finding a visible light active catalyst. The particles were characterized in their ability to photocatalytically degrade acetaldehyde in the gas phase under illumination with ultraviolet as well as with visible light. Furthermore, the measured activities are compared to those of well-known, titanium dioxide-based commercial standards.

Experimental section

Synthesis

Transition metal-modified zinc oxide was prepared using a facile sol–gel method. In a typical preparation, 60 mmol zinc acetate dihydrate (99.5 %, Carl Roth GmbH, Germany) was suspended in 200 mL of ethanol (99.8 %, Carl Roth GmbH, Germany). To stabilize the suspension, 20 mL of a complexing solution consisting of 3 mol L^{-1} diethanolamine (99 %, Sigma-Aldrich, USA) and 3 mol L^{-1} water in ethanol was added dropwise to the suspension, resulting in a clear solution. This solution was aged for 24 h under ambient conditions, and the resulting gel was subsequently transferred into a furnace for calcination. The calcination was conducted under air with the applied temperature program being as follows: heating up to 100°C with 2 $Kmin^{-1}$, maintaining at 100°C for 60 min, heating up to 500°C with 2 $Kmin^{-1}$, maintaining at 500°C for 300 min, and subsequently cooling to room temperature with 2 $Kmin^{-1}$. Eventually, the obtained powders were ground in an agate mortar. For the preparation of the transition metal-modified zinc oxides, a fraction of the zinc acetate dihydrate was substituted by the corresponding transition metal salt. The following salts were used as source materials for the corresponding transition metals: cobalt(II) acetate tetrahydrate (reagent grade), copper(II) acetate monohydrate (99 %), iron(II) acetate (95 %), manganese(II) acetate tetrahydrate (99 %), nickel(II) acetate tetrahydrate (99 %), ruthenium(III) acetylacetonate (97 %), titanium(IV) isopropoxide (97 %), and zirconium(IV) acetate (98 %) (Sigma-Aldrich, USA).

Acetaldehyde degradation

Measurements of photonic efficiency for the degradation of acetaldehyde were carried out on the basis of the ISO standard 22197-2. Samples of the zinc oxide powders were pressed into a 5×10 cm^2 acrylic glass molding with a resulting uniform and planar powder surface with an area of 3.926×10^{-3} m^2. These moldings were placed in an acrylic glass reactor with a laminar volume flux of 1.675×10^{-5} m^3s^{-1} with an acetaldehyde concentration of 1 ppm. The acetaldehyde concentration in the outlet gas flow was monitored using a Spectras GC955 gas chromatograph (Syntech, Netherlands) with a PID detector. Each sample was measured in the dark until an equilibrium concentration was reached and afterwards under illumination until an equilibrium concentration was reached. For the irradiation with ultraviolet (UV) light, a Cleo Compact (Philips, Netherlands) light source in combination with a LC-HU02 bandpass filter (Laser Components GmbH, Germany) was used so that no light with wavelengths above 400 nm remained. The resulting photon flux was determined using ferrioxalate actinometry (Parker 1953; Hatchard and Parker 1956) and was found to be 1.121×10^{-5}E s^{-1} m^{-2}. To measure degradation under visible light (VIS) irradiation, a 500-W halogen lamp with a LC-Y420 420-nm cutoff filter (Laser Components GmbH, Germany) was employed. The photon flux was determined to be 8.609×10^{-5} E s^{-1} m^{-2}, of which less than 0.1 % had a wavelength below 400 nm. So the measurements done with this irradiation setup can be considered to be exclusively visible light. Finally, the photonic efficiency ξ, which depicts the ratio of degraded molecules to impinging photons, was calculated according to the following formula:

$$\xi = \frac{(c_d - c_i)\cdot \dot{V}\cdot p}{\phi \cdot A \cdot R \cdot T}$$

where ξ is the photonic efficiency, c_d the acetaldehyde concentration under dark conditions, c_i the acetaldehyde concentration under illumination, $\dot{V}$ the volume flux, p the pressure, A the irradiation area, R the gas constant, T the absolute temperature, and ϕ the photon flux as determined by actinometry.

Scanning electron microscopy

Scanning electron micrographs were collected on a JSM-6700F (JEOL, Japan) with a cold cathode electron gun and a SEI detector for high resolution as well as a LEI detector. The powders were fixed on a conducting graphite block, and the micrographs were taken at an accelerating voltage of 2 kV and a working distance of 3 to 8 mm.

X-ray diffraction

X-ray diffraction (XRD) spectra were collected on a STADI P diffractometer (STOE, Germany) with a positional sensitive detector using monochromatic CuKα radiation. Average volume-weighted grain sizes were determined from the peak broadening using the Scherrer equation.

BET surface

The BET surface area of the samples was determined using a FlowSorb II 2300 (Micromeritics, USA) with a 30 % nitrogen/70 % helium gas mixture as adsorbate.

Diffuse reflectance and optical band gap

Diffuse reflectance spectra were collected on a Cary 4000 UV–visible spectrophotometer (Varian, USA) with an integrating sphere. The powders were fixed in a sample holder with a quartz window and measured against a polytetrafluoroethylene standard. The measured reflectance was transformed using the Kubelka-Munk function $F(R)$ to yield approximate absorption spectra of the samples. Furthermore, the resulting absorption spectra were used to construct Tauc plots ($(F(R)\cdot h\nu)^2$ vs $h\nu$) to allow the determination of the optical band gap. The optical band gap corresponds to the intercept of the extrapolated linear region with the energy axis.

Results

Transition metal-modified zinc oxide was prepared using a simple sol–gel method. The transition metals used were cobalt, copper, iron, manganese, nickel, ruthenium, titanium, and zirconium, and for each, a sample with 0.01, 0.1, and 1 at.% was synthesized.

While the synthesized zinc oxide powders were white to light gray in color, several of the samples of modified zinc oxide displayed a distinct color. Adding manganese turned the powders brown, cobalt green to turquoise, iron yellow to orange, and ruthenium dark green. The addition of nickel, zirconium, copper, or titanium in the studied concentration range had no effect on the color of the powder samples.

The samples were confirmed to be pure hexagonal zinc oxide by XRD (see Fig. 1). No other crystalline phases could be detected in the samples, except for the 1 at.% Ru-modified sample which contained a small amount of crystalline RuO_2. Also, neither homogeneous nor inhomogeneous lattice strain was detected in the diffractograms. Scanning electron microscopy (SEM) revealed that the powders consisted of roughly spherical particles with a diameter of 30–80 nm (see Fig. 2). This is in good agreement with the grain size of 56±6 nm determined by XRD. The BET surface was unexpectedly low at 6.26 $m^2\ g^{-1}$ and was attributed to aggregation of the particles and thus partial blocking of adsorption sites. The addition of transition metals in the studied concentration range did not have any significant effect on the morphology, size, or surface area of the particles.

The photocatalytic activities of the samples under irradiation with ultraviolet light are shown in Fig. 3. The photonic

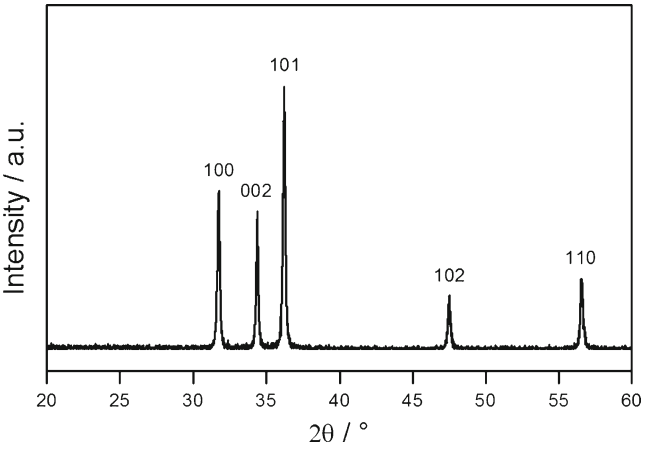

Fig. 1 XRD spectrum of the prepared zinc oxide particles (without modification). The corresponding crystal faces of hexagonal zinc oxide are depicted above the peaks

efficiency of zinc oxide could be improved by adding any of the studied transition metals, with the exception of nickel. In order of decreasing activity, the highest activity was achieved with Ru>Fe≈Cu>Ti>Co≈Mn≈Zr>pristine ZnO>Ni. In all cases, the highest activity was either measured with the 0.01 or the 0.1 at.% sample; the 1 at.% sample always displayed the lowest activity.

The measurements of the photonic efficiencies under irradiation with visible light revealed that only the ruthenium- and manganese-modified samples are capable of visible light photocatalysis; the visible light activity of the other samples was below the detection limit of the method. Therefore, only these materials were studied in more detail, and additional samples were synthesized to study the behavior over a wider concentration range.

In Fig. 4, the results for the detailed photocatalytic activity study of Mn-modified zinc oxide are presented. The maximum in photonic efficiency under illumination with ultraviolet light

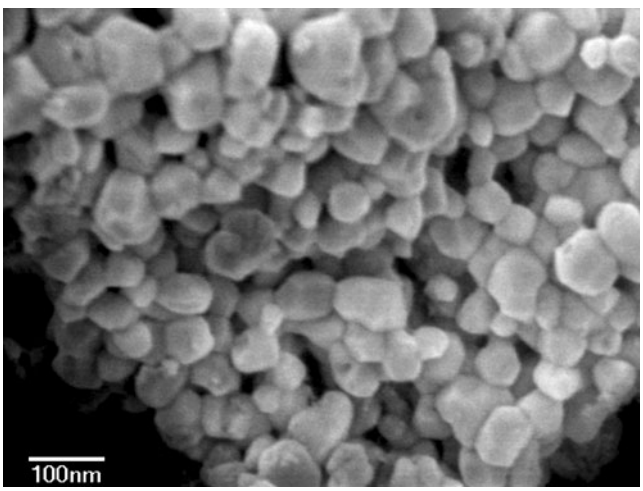

Fig. 2 SEM micrograph of the prepared zinc oxide particles (without modification)

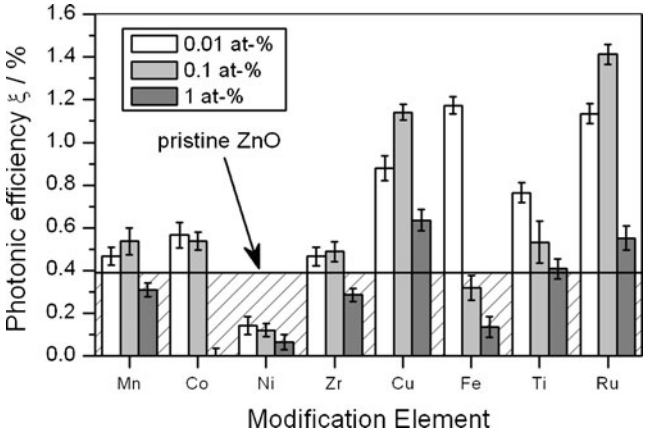

Fig. 3 Overview of the photocatalytic activity for the degradation of acetaldehyde under irradiation with ultraviolet light. Samples with 0.01 at.% (*white bars*), 0.1 at.% (*light gray bars*), and 1 at.% (*dark gray bars*) modification ratio as well as the value for pristine zinc oxide (*solid line*)

is reached at 0.1 at.% Mn modification. A higher concentration of Mn leads to a decrease in activity, and at ≥3 at.% Mn, no UV activity was observed at all. However, the photocatalytic activity under irradiation with visible light steadily increased with higher manganese content. The maximum in VIS activity was reached at 3 at.% Mn, and further addition of Mn did not result in a higher activity. The highest measured VIS photonic efficiency (0.039 %) was about one order of magnitude lower than the UV photonic efficiency of pristine zinc oxide (0.389 %).

Figure 5 shows the measured photonic efficiencies for the ruthenium-modified samples. Adding 0.01 at.% of ruthenium to zinc oxide increased the UV activity almost threefold. Higher Ru content increased the activity even further until a maximum was reached at 0.1 at.% Ru. More than 0.1 at.% ruthenium decreased the activity again. However, the 1 at.% Ru sample still showed a higher UV activity than the unmodified zinc oxide. This behavior is similar to the one displayed under

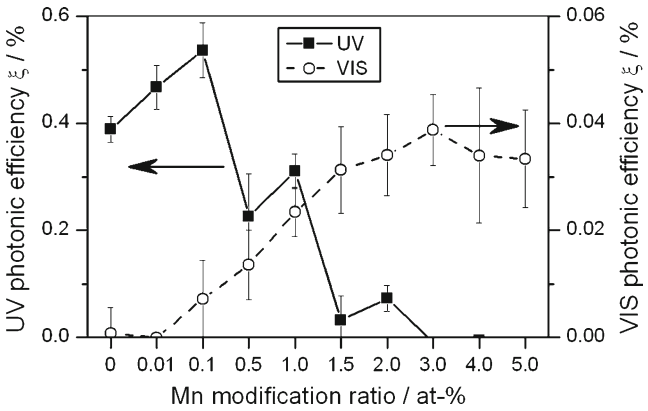

Fig. 4 The photocatalytic activity of Mn-modified ZnO samples for the degradation of acetaldehyde under (*solid line with black squares*) irradiation with UV light and (*dashed line with white circles*) irradiation with VIS light in relation to the Mn modification ratio

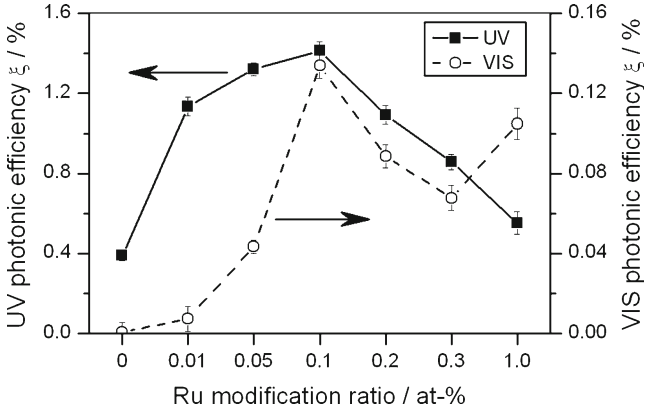

Fig. 5 The photocatalytic activity of Ru-modified ZnO samples for the degradation of acetaldehyde under (*solid line with black squares*) irradiation with UV light and (*dashed line with white circles*) irradiation with VIS light in relation to the Ru modification ratio

illumination with visible light. The VIS activity first rises with increasing Ru content until a maximum is reached at 0.1 at.% Ru with decreasing activity at higher Ru concentrations. The highest measured VIS photonic efficiency (0.134 %) was about a third of the UV photonic efficiency of pristine zinc oxide.

To put these values into perspective, some commercial photocatalysts have also been measured under the same conditions. The widely used Evonik Degussa Aeroxide P25 displayed a UV photonic efficiency of 1.47 %, which is slightly higher than that of our best sample (0.1 at.% Ru, 1.41 % photonic efficiency). Toho PP10 and Kronos vlp 7001 were used as standards for visible light photocatalysts. Their displayed VIS photonic efficiencies of 0.115 and 0.076 %, respectively, are higher than that of our best Mn-modified sample (3 at.% Mn, 0.039 % photonic efficiency) but lower than that of our best Ru-modified sample (0.1 at.% Ru, 0.134 % photonic efficiency).

The results of the diffuse reflectance measurements of the Mn- and Ru-modified samples are shown in Figs. 6 and 7, respectively. The Mn-modified samples show an increased absorption in the 400–500-nm region, corresponding to 2.5–3.1 eV photon energy. The absorption increases with increasing manganese content until it reaches a plateau at 3 at.%. The optical band gap of the samples was unchanged by the modification and was determined at 3.27 eV. Ru-modified samples exhibit a slightly increased absorption in the 400–550-nm region and an additional absorption peak at about 800 nm, corresponding to a photon energy of 1.55 eV. The optical band gap of the samples is unaffected by the Ru modification as well and is constant at 3.27 eV.

Discussion

Using a simple sol–gel technique, powder samples of zinc oxide modified with different transition metals were successfully prepared. For each metal, samples with 0.01, 0.1,

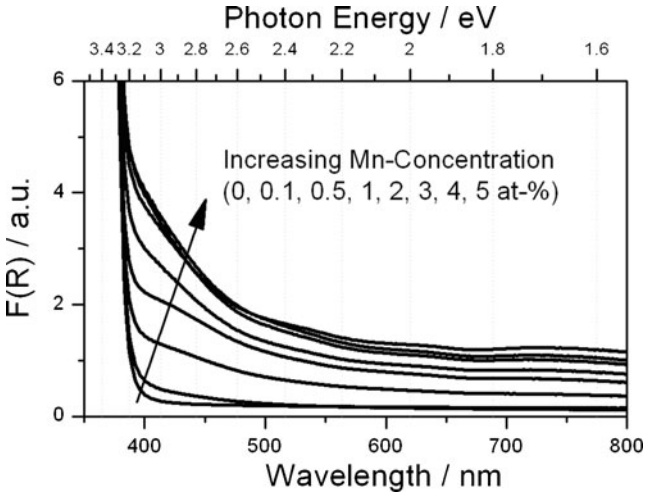

Fig. 6 Kubelka-Munk absorption of the Mn-modified zinc oxide samples calculated from diffuse reflectance measurements. The corresponding photon energies are displayed on the *upper x-axis*

and 1 at.%, respectively, were prepared. Due to the conditions applied (calcination in air at 500°C), the oxidation state of the metal ions present in the samples may not necessarily be identical to that of the initial compounds used. At this point, we do not know whether the transition metal ions are incorporated into the host lattice (doping), are adsorbed at the surface, or are present as entirely separate particles. However, no indication for the latter possibility was found in the SEM measurements.

While the main subject of this investigation is the visible light photoactivity, we also studied the behavior of the samples under ultraviolet irradiation since there is no detailed study with a standardized test system available yet. The results of the UV activity measurements suggest that an optimal concentration exists with a maximum in photonic

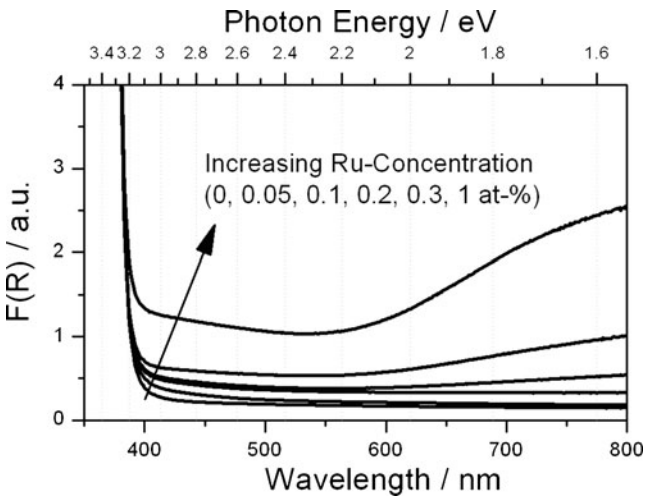

Fig. 7 Kubelka-Munk absorption of the Ru-modified zinc oxide samples calculated from diffuse reflectance measurements. The corresponding photon energies are displayed on the *upper x-axis*

efficiency for each modification element. In the case of copper and ruthenium, this optimal concentration seems to lie somewhere in the concentration range of 0.01–1 at.%. In case of titanium and iron, the optimum seems to be located somewhere below 0.1 at.%, possibly even lower than 0.01 at.%. However, the results for manganese, cobalt, nickel, and zirconium are inconclusive concerning the position of the optimal modification ratio.

To explain this behavior, the mechanism of charge separation in photocatalysis has to be considered. One of the possibilities to achieve better charge separation is by doping the host material with metal ions (M^{n+}) in order to create electron and/or hole traps (Choi et al. 1994).

$$M^{n+} + e_{cb}^{-} \rightarrow M^{(n-1)+} \quad \text{electron trap}$$

$$M^{n+} + h_{vb}^{+} \rightarrow M^{(n+1)+} \quad \text{hole trap}$$

These traps will immobilize the charge carriers and thus reduce the recombination rate. While trapped charge carriers may also recombine through tunneling, their recombination rate is usually several orders of magnitude lower than that of free charge carriers.

This is in accordance with the results obtained in this study. Adding even very small amounts of transition metals to the zinc oxide particles increased their activity in all cases studied except for nickel. Using this approach, the photonic efficiency under irradiation with ultraviolet light could be increased up to 3.6-fold in comparison with unmodified zinc oxide (by adding 0.1 at.% Ru).

However, while metal ion dopants in the host zinc oxide lattice may act as charge carrier traps and thus reduce the rate of recombination, they may also act as recombination centers if the dopant concentration gets too high. The rate of recombination through tunneling between trapped charge carriers increases exponentially with decreased distance between the centers. Consequently, the most extreme case, when one dopant is in direct cationic neighborhood to another dopant, may be considered a recombination center. More distant dopants lead to several orders of magnitude lower recombination rates and may be disregarded in this model. The statistical probability p for such an event in a wurtzite lattice (12 cationic neighbors) is directly dependent on the doping ratio r_d:

$$p = 1 - (1 - r_d)^{12}$$

However, not only the cluster probability increases with the doping ratio but also the total number of dopant atoms. The ratio of clusters to total cations r_c can be expressed as:

$$r_c = r_d \cdot p = r_d \cdot \left(1 - (1 - r_d)^{12}\right)$$

As can be seen in Fig. 8, the cluster ratio increases exponentially with the doping ratio. While the cluster ratio

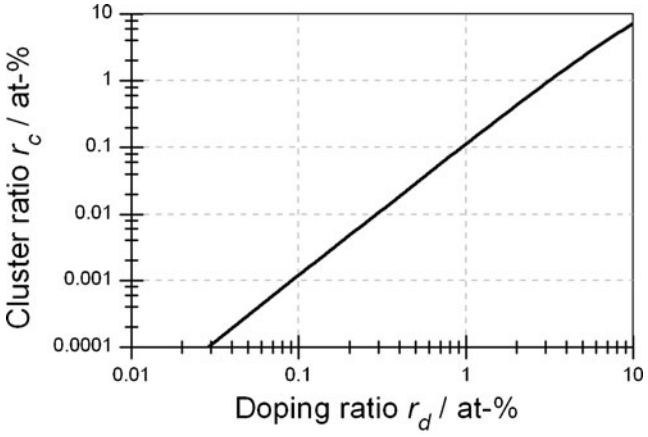

Fig. 8 Ratio of clusters r_c to total cations as a function of the doping ratio r_d. Clusters are dopant atoms having another doping atom as a direct neighbor in a wurtzite lattice

is quite insignificant (<1 ppm) at doping ratios below 0.03 at.%, already every thousandths cation is a recombination center at a doping ratio of 1 at.%. At the highest doping ratio studied in this work, 5 at.%, the cluster ratio is at 2.3 at.% according to this model, which would mean that almost every second dopant acts as a recombination center. Even though it may be doubtful that such high dopant concentrations are actually incorporated into the host lattice due to solubility limits, these calculations can be taken as an explanation for the low photocatalytic activities of the samples with a high content of foreign atoms.

A similar study on doped TiO_2 by Choi et al. in 1994 also reported an optimal doping concentration with higher doping ratios resulting in a decline of the photocatalytic activity. The observed optimal doping concentration of 0.5 at.% is higher than in our work. However, much smaller particles (2–4 nm) were used in this study corresponding to only one to five doping atoms per particle (Choi et al. 1994). As the particles used in the present study are much larger (about 50 nm), the dopant concentration may be significantly lower without creating "empty" particles not containing a single dopant atom. This also suggests that the optimal doping ratio may be dependent not only on the nature of the dopant but also on the morphology and size of the particles. This was also proposed by Zhang et al. (1998) who concluded that the optimal Fe^{3+}-doping ratio for TiO_2 was dependent on the particle size. The varying optimal modification concentration for the elements studied may be attributed to different solubilities in the host lattice so that not the same amount of every metal was incorporated into the zinc oxide for a given modification ratio.

For titanium, zirconium, and ruthenium, charge compensation is also an issue, since they have a higher valence than zinc. If they are incorporated into the zinc oxide lattice, their excess positive charge could be compensated by zinc vacancies or less oxygen vacancies, which are inherently present in zinc oxide.

Modification with nickel seemed to be detrimental for the photocatalytic activity. Adding even a very small amount (0.01 at.%) would decrease the activity by a factor of 2.7. This is in accordance with findings from Kaneva et al. (2011) who also reported a decrease in activity with nickel-doped zinc oxide but studied a higher concentration regime.

The measurements of photocatalytic activity also showed that out of all studied elements, only manganese and ruthenium were able to produce visible light active modified zinc oxide. Consequently, these materials were studied more precisely. In addition to their performance under visible light, these studies also revealed the exact position of the optimal modification ratio for UV activity to be at 0.1 at.% for both cases.

We proposed that at high doping ratios, the foreign atoms act as recombination centers and thus reduce the photocatalytic activity. Therefore, it is curious that the manganese-modified samples show their highest visible light activity only at very high modification ratios of 3–5 at.%. However, since there was neither a change in the band gap nor any homogeneous or inhomogeneous lattice strain in the XRD, it is unlikely that the majority of the foreign atoms were incorporated into the host lattice in this case. As there was also no crystalline manganese– or zinc–manganese species detected, we propose that while a small amount might still be embedded inside the zinc oxide, the majority of the manganese is instead absorbed on the surface of the zinc oxide particles.

If the manganese is adsorbed on the surface, the visible light activity of the Mn-modified samples can be explained by a direct interfacial charge transfer mechanism as proposed by Irie et al. (2008). In their proposed mechanism, electrons are excited directly from the valence band of the semiconductor to the adsorbed metal ions. The energy of the absorbed photons corresponds to the potential difference between the valence band and the redox potential of the metal ion plus their reorganization energy. The reduced metal ions can subsequently reduce oxygen via a two- or four-electron transfer, depending on the redox potential of the absorbed species (Nosaka et al. 2011). This effect was observed with Cu(II)-grafted WO_3 and TiO_2 as well as with Fe(III)-grafted TiO_2 (Irie et al. 2008; Yu et al. 2010). The additional absorption of the Mn-modified ZnO samples in the range of 400–500 nm corresponds to about 2.5–3.1 eV of photon energy, suggesting that the redox potential of the adsorbed Mn species is in the range of −0.2 to +0.4 V vs SHE. The absorption is also proportional to the visible light activity, which can be taken as further confirmation for this theory. Figure 9 depicts the proposed mechanism of the visible

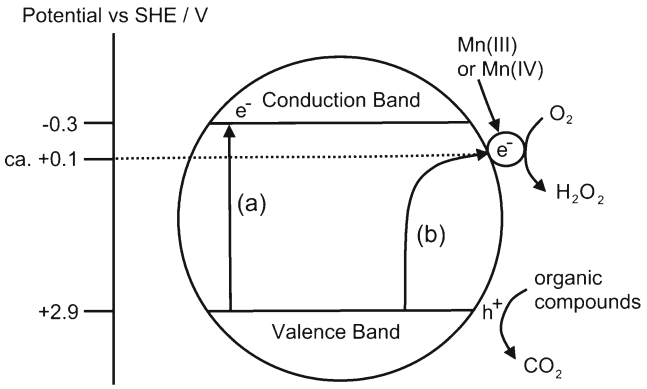

Fig. 9 Proposed mechanism for direct interfacial charge transfer. Photon absorption leads to (*a*) electron promotion to the conduction band of ZnO (E=3.2 eV; λ=388 nm) or (*b*) direct interfacial electron transfer to surface-bound Mn(III) or Mn(IV) species (E=~2.8 eV; λ=~443 nm)

light-inducted interfacial charge transfer for Mn-modified ZnO. The adsorbed manganese species is most likely either a Mn(III)/Mn(IV) or a Mn(II)/Mn(III) redox couple. However, further studies are necessary to exactly identify the species in question and its redox potential.

Also, it was shown that Mn_2O_3/C electrodes act similar to Pt/C electrodes and catalyze a four- or quasi-four-electron transfer to oxygen (Cheng et al. 2009). This further suggests that this mechanism involves a multi-electron oxygen reduction, with the corresponding more positive potentials at +0.68 and +1.23 V for the two- and four-electron reduction, respectively (Irie et al. 2008).

The visible light activity of the Ru-modified samples may also be explained by the direct interfacial charge transfer, although the results are less clear here. Further investigations are required to explain this phenomenon.

This mechanism may not work with the other metals studied since the redox potential of the species in question has to fit well inside the band gap of the semiconductor. Also, the reduced species needs to be able to reduce molecular oxygen via a multi-electron transfer. Also, the synthesis conditions might not be optimal to produce adsorbed species on zinc oxide for the other metals studied.

Besides this interfacial charge transfer mechanism, it may also be possible that there are impurity energy levels created by transition metal doping that lie inside the band gap (Rehman et al. 2009). The corresponding energy required for the excitation would be smaller than the band gap energy and thus corresponding to visible light. A narrowing of the band gap, however, could not be observed. This would further indicate that no or only a small percentage of the manganese ions were integrated into the host lattice, as this is known to alter the band gap (Wang et al. 2006; Ekambaram et al. 2007). Further studies of these materials will clarify which of these possible mechanisms is occurring.

One interesting result is also that some of the Mn-modified samples seem to have photocatalytic activity exclusively under visible light irradiation. These results fit well with the proposed mechanism as electron/hole pairs created by ultraviolet irradiation would most likely recombine through one of the many recombination centers. Visible light irradiation, though, would induce interfacial charge transfer and proceed to react with surface-absorbed oxygen. However, the measured VIS activity of the Mn-modified samples is rather small and thus barely above the detection limit of the conditions employed in the UV activity measurements. Hence, further investigations are necessary to confirm that there is indeed less activity under ultraviolet than under visible light irradiation.

Conclusions

It was shown that, albeit the UV photocatalytic activity of unmodified zinc oxide is much smaller than that of titanium dioxide, it can be increased up to the same level by adding small amounts of transition metals such as Cu, Fe, Ru, or Ti. The photocatalytic activity of transition metal-modified zinc oxide is explained by the formation of traps at lower dopant concentrations and the formation of recombination centers at higher dopant concentrations, respectively. The optimal dopant concentration depends on the nature of the dopant and may also depend on the morphology and size of the particles. The maximum in UV activity was achieved using doping concentrations in the range of 0.01 to 0.1 at.%. Mn- and Ru-modified zinc oxides also display photocatalytic activity under visible light irradiation. While for Mn modification the UV activity decreases with increasing VIS activity, with Ru modification, the UV and VIS activities both have their maximum at the same Ru concentration, 0.1 at.%.

While manganese-modified zinc oxide has been studied and described before, the ruthenium-modified zinc oxide is a novel and highly active material for visible light photocatalysis. The VIS activity of Ru-modified zinc oxide even surpasses that of the best titania-based visible light photocatalyst used as standard (Toho PP10) by up to 17 %. This is especially remarkable since the surface area of the sample is very small when compared to those of the titania catalysts. This indicates that Ru-modified zinc oxide may be a suitable alternative to titanium dioxide-based catalysts. The observed activity under visible light irradiation can be explained by the direct interfacial charge transfer of valence band electrons to adsorbed metal ions. The reduced metal ions may then reduce molecular oxygen, most likely in a multi-electron reaction. However, the exact nature of the visible light activity will be subject to further investigations.

Acknowledgments Financial support by the German Federal Ministry of Education and Research (BMBF Project "HelioClean," grant no. 03X0069F) is gratefully acknowledged.

References

Cheng F, Shen J, Ji W, Tao Z, Chen JC (2009) Selective synthesis of manganese oxide nanostructures for electrocatalytic oxygen reduction. ACS Appl Mater Interf 1:460–466. doi:10.1021/am800131v

Choi W, Termin A, Hoffmann MR (1994) The role of metal ion dopants in quantum-sized TiO2: correlation between photoreactivity and charge carrier recombination dynamics. J Phys Chem 98:13669–13679

Ekambaram S, Iikubo Y, Kudo A (2007) Combustion synthesis and photocatalytic properties of transition metal-incorporated ZnO. J Alloys Compd 433:237–240. doi:10.1016/j.jallcom.2006.06.045

Hatchard CG, Parker CA (1956) A new sensitive chemical actinometer. II. Potassium ferrioxalate as a standard chemical actinometer. Proc R Soc A 235:518–536

Herrmann J-M (2005) Heterogeneous photocatalysis: state of the art and present applications. Top Catal 34:49–65. doi:10.1007/s11244-005-3788-2

Irie H, Miura S, Kamiya K, Hashimoto K (2008) Efficient visible light-sensitive photocatalysts: grafting Cu(II) ions onto TiO_2 and WO_3 photocatalysts. Chem Phys Lett 457:202–205. doi:10.1016/j.cplett.2008.04.006

Kanade KG, Kale BB, Baeg J-O, Lee SM, Lee CW, Moon SJ, Chang H (2007) Self-assembled aligned Cu doped ZnO nanoparticles for photocatalytic hydrogen production under visible light irradiation. Mater Chem Phys 102:98–104. doi:10.1016/j.matchemphys.2006.11.012

Kaneva NV, Dimitrov DT, Dushkin CD (2011) Effect of nickel doping on the photocatalytic activity of ZnO thin films under UV and visible light. Appl Surf Sci 257:8113–8120. doi:10.1016/j.apsusc.2011.04.119

Nosaka Y, Takahashi S, Sakamoto H, Nosaka AY (2011) Reaction mechanism of Cu(II)-grafted visible-light responsive TiO_2 and WO_3 photocatalysts studied by means of ESR spectroscopy and chemiluminescence photometry. J Phys Chem C 115:21283–21290. doi:10.1021/jp2070634

Parker CA (1953) A new sensitive chemical actinometer. I. Some trials with potassium ferrioxalate. Proc R Soc A 220:104–116

Rehman S, Ullah R, Butt AM, Gohar ND (2009) Strategies of making TiO_2 and ZnO visible light active. J Hazard Mater 170:560–569. doi:10.1016/j.jhazmat.2009.05.064

Ullah R, Dutta J (2008) Photocatalytic degradation of organic dyes with manganese-doped ZnO nanoparticles. J Hazard Mater 156:194–200. doi:10.1016/j.jhazmat.2007.12.033

Wang YS, Thomas PJ, O'Brien P (2006) Optical properties of ZnO nanocrystals doped with Cd, Mg, Mn, and Fe ions. J Phys Chem B 110:21412–21415. doi:10.1021/jp0654415

Xiao Q, Zhang J, Xiao C, Tan X (2007) Photocatalytic decolorization of methylene blue over Zn1-xCoxO under visible light irradiation. Mater Sci Eng B 142:121–125. doi:10.1016/j.mseb.2007.06.021

Yu H, Irie H, Shimodaira Y, Hosogi Y, Kuroda Y, Miyauchi M, Hashimoto (2010) An efficient visible-light-sensitive Fe(III)-grafted TiO_2 photocatalyst. J Phys Chem C 114:16481–16487. doi:10.1021/jp1071956

Zhang D (2012) Structural, optical, electrical, and photocatalytic properties of manganese doped zinc oxide nanocrystals. Rus J Phys Chem A 86:93–99. doi:10.1134/S0036024412010086

Zhang Z, Wang C-C, Zakaria R, Ying JY (1998) Role of particle size in nanocrystalline TiO_2-based photocatalysts. J Phys Chem B 102:10871–10878. doi:10.1021/jp982948+